

## Harmonic quantum heat devices: Optimum-performance regimes

N. Sánchez-Salas\* and A. Calvo Hernández

*Departamento de Física Aplicada, Facultad de Ciencias, Universidad de Salamanca, 37008 Salamanca, Spain*

(Received 13 May 2004)

The finite-time performance of a quantum-mechanical heat engine (or refrigerator) with a working fluid consisting of many noninteracting harmonic oscillators is considered in order to analyze three optimum operating regimes: maximum efficiency (maximum coefficient of performance), maximum work output (maximum cooling load) and a third one,  $\Omega$  criterion, which represents a compromise between them. The reported results extend previous findings for macroscopic and mesoscopic energy converters to quantum heat devices and also endorse the  $\Omega$  criterion as a unified, optimum working regime for energy converters, independent of their size and nature.

DOI: XXXX

PACS number(s): 05.70.-a, 07.20.Pe

### I. INTRODUCTION

In the context of finite time thermodynamics [1,2], we have reported a unified optimization criterion (hereafter referred to as  $\Omega$  criterion) for energy converters in nonideal processes [3]. If the process is characterized by an appropriate independent variable  $y$  and a set of parameters, or controls,  $\{\gamma\}$ , we define the  $\Omega$  criterion as a way to evaluate the best compromise between effective useful energy  $E_{u,eff}(y; \{\gamma\})$  and lost useful energy  $E_{u,L}(y; \{\gamma\})$ . Specifically, we take the  $\Omega$  function as the difference between these energies, i.e.,  $\Omega(y; \{\gamma\}) \equiv E_{u,eff}(y; \{\gamma\}) - E_{u,L}(y; \{\gamma\})$ . Results for irreversible models of macroscopic thermal devices (heat engines and refrigerators) with both linear and nonlinear heat transfer laws [3,4], isothermal linear models of biological motors [3], nonlinear systems rectifying thermal fluctuations [5,6], and adiabatic rocking ratchets [7], show that in all cases the  $\Omega$ -based operation regime is intermediate between those arising from maximum useful energy (power output in heat engines and cooling power in refrigerators) and from maximum efficiency [coefficient of performance (COP) in refrigerators]. Moreover, the application of this criterion is independent of environmental parameters (usually difficult to estimate) and does not require the explicit evaluation of entropy generation (a subtle issue in most cases) [2,8]. Its implementation to heat engines only requires the knowledge of power output  $P$  and efficiency  $\eta$ , while in the case of refrigerators the cooling power  $Q_L$  and COP  $\epsilon$  are needed. In these cases it reads as [see Eqs. (2) and (3) in Ref. [3]]

$$\Omega^{HE}(y; \{\gamma\}) = \frac{2\eta(y; \{\gamma\}) - \eta_{max}(\{\gamma\})}{\eta(y; \{\gamma\})} P(y; \{\gamma\}) \quad (1)$$

and

---

\*Also at Departamento de Física, Escuela Superior de Física y Matemáticas, Instituto Politécnico Nacional, Edif. No. 9, U. P. Zacatenco, 07738 México D. F., México.

$$\Omega^{RE}(y; \{\gamma\}) = \frac{2\epsilon(y; \{\gamma\}) - \epsilon_{max}(\{\gamma\})}{\epsilon(y; \{\gamma\})} Q_L(y; \{\gamma\}), \quad (2)$$

where  $\eta_{max}(\{\gamma\})$  and  $\epsilon_{max}(\{\gamma\})$  are the maxima of the efficiency and COP, respectively, in the allowed range of values of  $y$  for given  $\gamma$ 's.

On the other hand, the investigation relative to quantum cycle models (for both heat engines and refrigerators), their high temperature limit, and the nature of the working substance has attracted a great deal of attention in the last years (see, for example, Refs. [9–13] and cites therein). Along this line, the main goal of this brief paper is to extend the previous studies [3–7] on optimum working regimes (in particular those on  $\Omega$  criterion) for macroscopic and mesoscopic systems to cycles with a quantum dynamics. With this aim, we consider in the following section a harmonic irreversible quantum cycle. Finally, we will face the obtained results to those reported for macroscopic, traditional, heat engines, and refrigerators and those reported for stochastic, ratchet devices in order to stress some unified behaviors of thermal devices, independent of their nature and size.

### II. HARMONIC QUANTUM CYCLES

Many models of quantum cycles with different working substances (such as harmonic oscillators, spin systems, and ideal quantum gases) have been worked out [9–13]. As a suitable model in our study we will consider in this paper an irreversible quantum cycle with a working medium consisting of many noninteracting harmonic oscillators. This model is completely analogous to the one reported by Feldman and Kosloff [12] for an ensemble of noninteracting two level systems, in which the internal irreversibilities are considered through a phenomenological friction coefficient  $\sigma$ , while the external irreversibilities comes from the coupling of the working medium with external thermal baths. These authors stressed in their analysis the optimum time allocation of the system in the different steps of the cycle, nevertheless we will focus here on an analysis of the above-mentioned three optimum-performance regimes for a constant total cycle time.

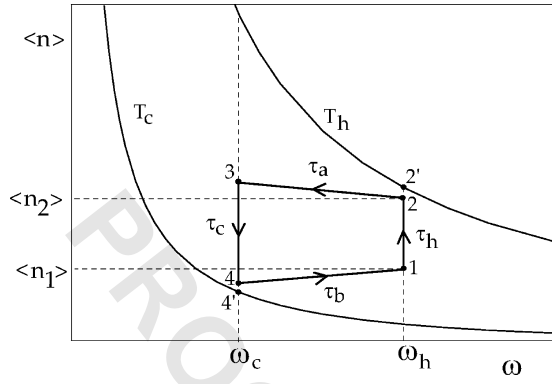


FIG. 1.  $\langle n \rangle$ - $\omega$  scheme of the harmonic quantum power cycle.

### A. Harmonic heat engine

A schematic view of the power cycle in the population-frequency ( $\langle n \rangle$ - $\omega$ ) diagram can be seen in Fig. 1. The working medium is coupled to a hot thermal bath of temperature  $T_h$  during a time  $\tau_h$  with a constant frequency  $\omega_h$  along the thermal branch  $1 \rightarrow 2$ , thus increasing its population from  $\langle n_1 \rangle$  to  $\langle n_2 \rangle$ . Along the *adiabatic* branch  $2 \rightarrow 3$  variations of the internal energy coming from a linear change both of the frequency and of the population (this induced by the internal friction coefficient  $\sigma$ ) during a time  $\tau_a$ . Along the third branch  $3 \rightarrow 4$  the system remains coupled to a cold thermal bath of temperature  $T_c$  during a time  $\tau_c$  with a constant frequency  $\omega_c$ , and lowering its population from  $\langle n_3 \rangle$  to  $\langle n_4 \rangle$ . In the last *adiabatic* branch  $4 \rightarrow 1$  the system closes the cycle changing again its internal energy by linear variations of the frequency and populations during a period  $\tau_b$ .

The energy balance of this cycle is the same that the one carried out with detail by Feldman and Kosloff [12] but substituting the polarization of the two level system by the populations of the harmonic oscillators and it will be not repeated here. The final results for the (dimensionless) net work output  $\bar{W}$  and absorbed heat from the hot thermal bath  $\bar{Q}_{abs}$  are given, respectively, by

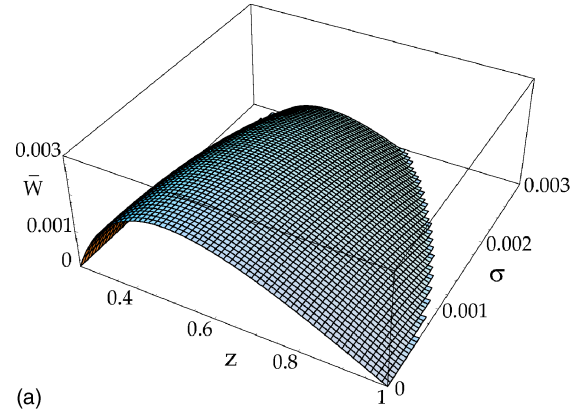
$$\begin{aligned} \bar{W} &\equiv \frac{W}{w_h} \\ &= (1-z)\Delta n^{eq}F(x,y) - \frac{\sigma^2}{1-xy} \\ &\quad \times \left[ z(1-x)\left(\frac{1}{\tau_a} + \frac{y}{\tau_b}\right) + \left(\frac{x}{\tau_a} + \frac{1}{\tau_b}\right)(1-y) \right] \end{aligned} \quad (3)$$

and

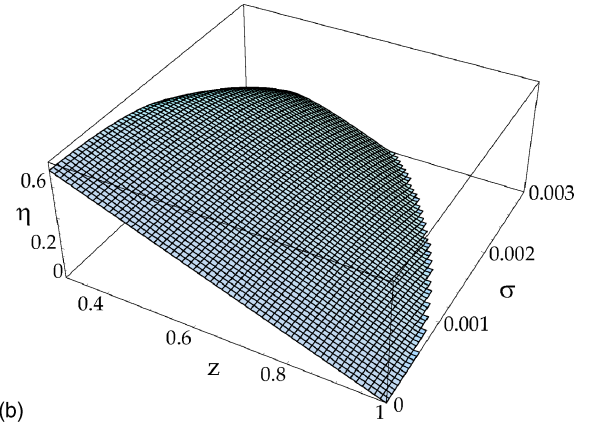
$$\bar{Q}_{abs} \equiv \frac{Q_{abs}}{w_h} = \Delta n^{eq}F(x,y) - \frac{\sigma^2(1-y)}{1-xy}\left(\frac{x}{\tau_a} + \frac{1}{\tau_b}\right), \quad (4)$$

where

$$\Delta n^{eq} = \frac{1}{\exp(\beta_h w_h) - 1} - \frac{1}{\exp(\beta_c w_c) - 1}, \quad (5)$$



(a)



(b)

FIG. 2. Harmonic quantum power cycle: (a) normalized work output  $\bar{W}$  and (b) efficiency  $\eta$ ,  $z$  and  $\sigma$ . In all cases  $\Gamma_c=1$ ,  $\Gamma_h=2$ ,  $\tau_h=\tau_c=\tau_a=\tau_b=0.01$ ,  $T_c=2000$ ,  $T_h=8000$ , and  $w_h=6000$ .

$$F(x,y) = \frac{(1-x)(1-y)}{1-xy}, \quad (6)$$

and

$$x = e^{-\Gamma_c \tau_c}, \quad y = e^{-\Gamma_h \tau_h}. \quad (7)$$

In the above equations  $\hbar=1$ ,  $k_B=1$ ,  $\beta=1/T$ , and  $\Gamma_c$  and  $\Gamma_h$  are constants associated to the relaxation of the working medium when is coupled to the cold and hot thermal baths, respectively.

Work output  $\bar{W}$  and efficiency  $\eta = \bar{W}/\bar{Q}_{abs}$  are shown in Fig. 2 versus  $z = (\omega_c/\omega_h)$  and  $\sigma$  for the indicated values of the (dimensionless) parameters accounting for the times in each branch ( $\tau_a, \tau_b, \tau_h, \tau_c$ ), the temperatures of the external thermal baths ( $T_h, T_c$ ), and the constants ( $\Gamma_h, \Gamma_c$ ). These figures show that both magnitudes decrease as the friction increases and that both of them are convex functions, thus showing maxima for some  $z$  values (the monotonic decreasing behavior of  $\eta$  on  $z$  when  $\sigma=0$  will be analyzed below). A closer inspection to Fig. 2 shows that for any  $\sigma$  the values of  $z$  giving maximum work and maximum efficiency are different [see Fig. 3(a)] and, as a consequence, the parametric work-efficiency plots show the characteristic looplike behavior of Fig. 3(b). Thus work output and efficiency are functions with maximum values in terms of  $z$ , which can be considered as

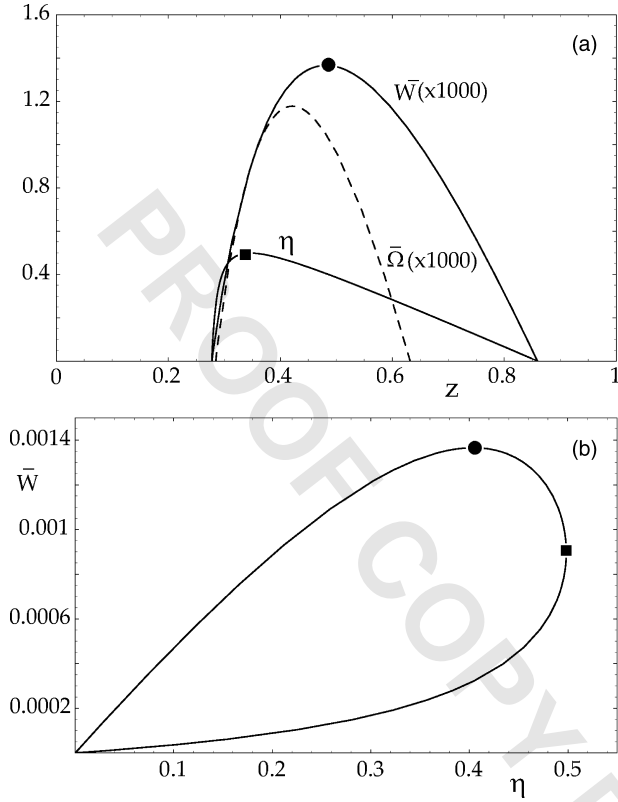


FIG. 3. Harmonic quantum power cycle: (a) normalized work output  $\bar{W}(\times 1000)$ , efficiency  $\eta$ , and  $\bar{\Omega}(\times 1000)$   $z$ ; (b) parametric behavior  $\bar{W} - \eta$ . In all cases  $\sigma=0.002$ ,  $\Gamma_c=1$ ,  $\Gamma_h=2$ ,  $\tau_h=\tau_c=\tau_a=\tau_b=0.01$ ,  $T_c=2000$ ,  $T_h=8000$ , and  $w_h=6000$ . The circle denotes the maximum work point and the square the maximum efficiency point.

an appropriate independent variable in a optimization procedure of these magnitudes and, as a consequence, of the function  $\Omega^{HE}$ , see Eq. (1) and Fig. 3(a). The results of this procedure in terms of  $\sigma$  are shown in Fig. 4: in Fig. 4(a) we plot the  $z$  values giving maximum efficiency  $z_{max\eta}$ , maximum work output  $z_{max\bar{W}}$ , and maximum  $\bar{\Omega}$   $z_{max\bar{\Omega}}$ ; in Fig. 4(b) we show maximum work  $\bar{W}_{max}$ , work under maximum efficiency  $\bar{W}_{max\eta}$  and under maximum  $\bar{\Omega}$   $\bar{W}_{max\bar{\Omega}}$ ; and Fig. 4(c) shows the maximum efficiency  $\eta_{max}$ , the efficiency under maximum work  $\eta_{max\bar{W}}$ , and under maximum  $\bar{\Omega}$  conditions  $\eta_{max\bar{\Omega}}$ . From plots in the figures we stress that the criterion  $\Omega^{HE}$  gives values of  $z$ ,  $\bar{W}$ , and  $\eta$  which are intermediate between those for maximum work and maximum efficiency performance criteria.

As noted before, the behavior of efficiency  $\eta$  with  $z$  when friction is absent ( $\sigma=0$ ) is a particular case. Under this condition  $\eta$  decreases monotonically on  $z$  from its maximum value to zero and the parametric work-efficiency plots become open curves similar to those found under the so called *endoreversible* conditions [1,3,14] (i.e., the only source of irreversibility is the coupling of the system to the external thermal baths). However, as stressed by Feldmann and Kosloff [12], this limit is only reached mathematically when  $\sigma=0$  and besides the high temperature limit is fulfilled:  $T_h \gg \omega_h$  and  $T_c \gg \omega_c$ . With these assumptions it is easy to obtain

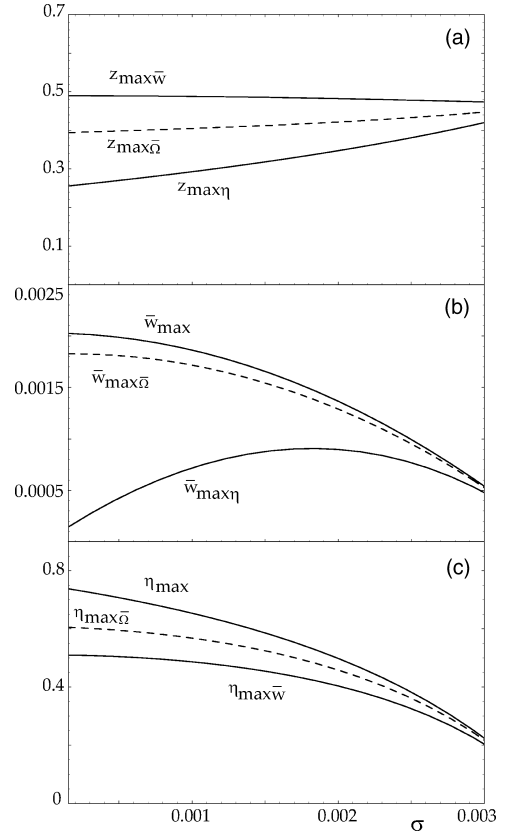


FIG. 4. Optimization results for the harmonic quantum power cycle: (a)  $z_{max\bar{W}}$ ,  $z_{max\bar{\Omega}}$ , and  $z_{max\eta}$ ; (b)  $\bar{W}_{max}$ ,  $\bar{W}_{max\bar{\Omega}}$ , and  $\bar{W}_{max\eta}$ ; (c)  $\eta_{max}$ ,  $\eta_{max\bar{\Omega}}$ , and  $\eta_{max\bar{W}}$ . In all cases  $\Gamma_c=1$ ,  $\Gamma_h=2$ ,  $\tau_h=\tau_c=\tau_a=\tau_b=0.01$ ,  $T_c=2000$ ,  $T_h=8000$ , and  $w_h=6000$ .

some known (and expected) values for the efficiency already reported for macroscopic and endoreversible heat engines with linear heat transfer laws: the efficiency under maximum work conditions is the well-known Curzon-Ahlborn value [1–3],  $\eta_{max\bar{W}}=1-\sqrt{\tau}(\tau=T_c/T_h)$ , and the efficiency under maximum  $\bar{\Omega}$  conditions is  $\eta_{max\bar{\Omega}}=1-\sqrt{\tau(\tau+1)}/2$ , an expression reported for endoreversible heat engines optimized under the ecological criterion [14].

## B. Harmonic refrigerator

Figure 5 shows a schematic  $\langle n \rangle - \omega$  diagram of the quantum harmonic refrigeration cycle: two thermal branches  $1 \rightarrow 2$  and  $3 \rightarrow 4$  where the working medium, respectively, absorbs heat from the cold thermal bath at temperature  $T_c$  and rejects heat to the hot thermal bath at temperature  $T_h$ , alternating with two *adiabatic* branches  $2 \rightarrow 3$  and  $4 \rightarrow 1$  in which the internal energy changes with both the populations and the frequency. In this case the magnitudes of interest are the (dimensionless) heat absorbed by the system from the cold thermal bath,  $\bar{Q}_L \equiv Q_L/w_h$ , and the work input to the system  $\bar{W}_{in} \equiv W_{in}/w_h$ , which are given, respectively, by

$$\bar{Q}_L = z \left[ -\Delta n^{eq} F(x, y) - \frac{\sigma^2(1-x)}{1-xy} \left( \frac{y}{\tau_a} + \frac{1}{\tau_b} \right) \right] \quad (8)$$

and

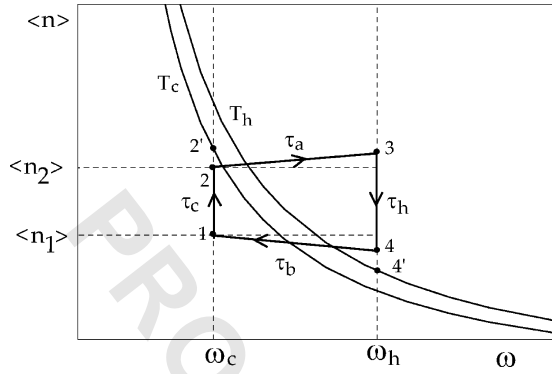


FIG. 5.  $\langle n \rangle$ - $w$  scheme of the harmonic quantum refrigeration cycle.

$$\begin{aligned} \bar{W}_{in} = & -(1-z)\Delta n^{eq}F(x,y) + \frac{\sigma^2}{1-xy} \left[ z(1-x) \left( \frac{y}{\tau_a} + \frac{1}{\tau_b} \right) \right. \\ & \left. + (1-y) \left( \frac{1}{\tau_a} + \frac{x}{\tau_b} \right) \right]. \end{aligned} \quad (9)$$

From the above magnitudes the COP is given by  $\epsilon = \bar{Q}_L / \bar{W}_{in}$  and the  $\Omega^{RE}$  function can be obtained from Eq. (2).

Three dimensional plots of  $\bar{Q}_L$  and  $\epsilon$  are shown in Figs. 6(a) and 6(b), respectively, versus  $z$  and  $\sigma$ . In these figures

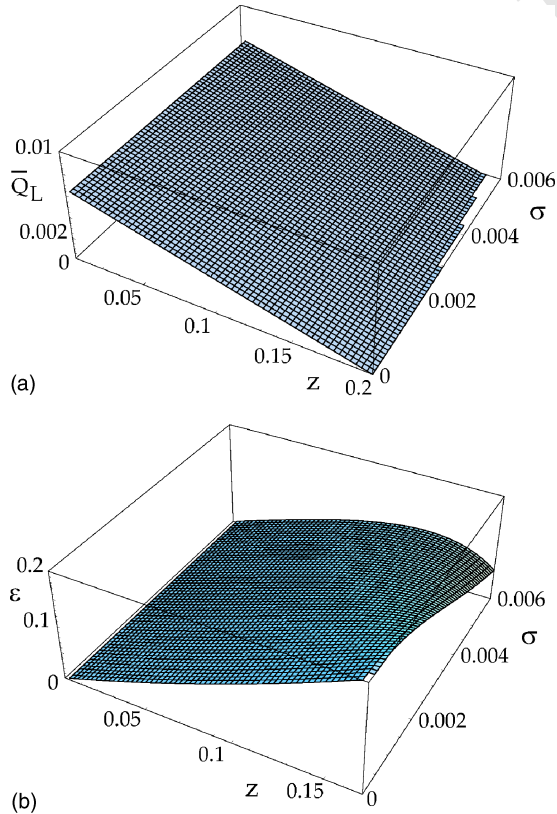


FIG. 6. Harmonic quantum refrigeration cycle: heat absorbed from the cold thermal bath  $\bar{Q}_L$  (a) and COP  $\epsilon$ , (b)  $z$  and  $\sigma$ . In both cases  $\Gamma_c=1$ ,  $\Gamma_h=2$ ,  $\tau_h=\tau_c=\tau_a=\tau_b=0.01$ ,  $T_c=100$ ,  $T_h=500$ , and  $w_h=100$ .

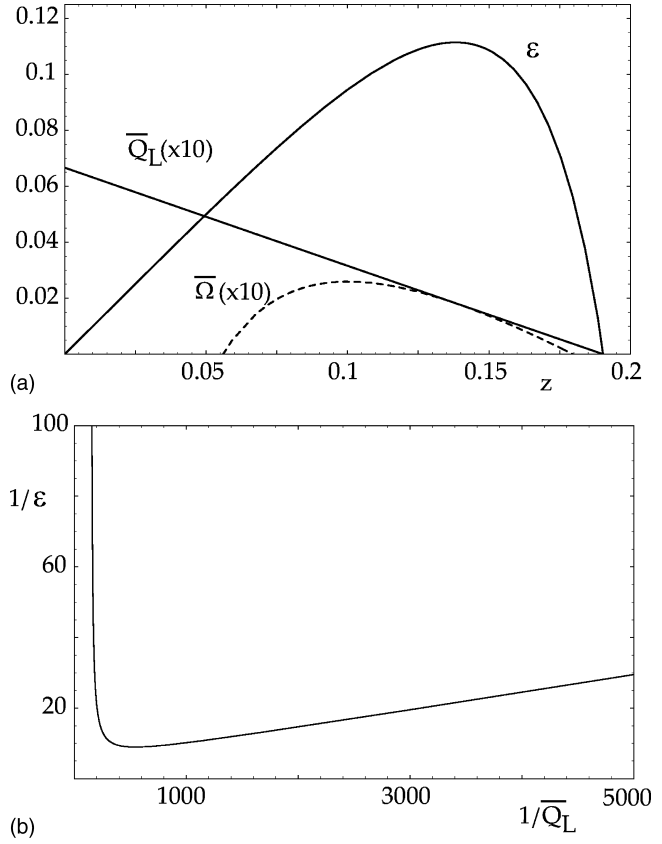


FIG. 7. Harmonic quantum refrigeration cycle: (a) heat absorbed from the cold thermal bath  $\bar{Q}_L (\times 10)$ , COP  $\epsilon$ , and  $\bar{\Omega} (\times 10)$  against  $z$ ; (b) parametric behavior  $1/\epsilon - 1/\bar{Q}_L$ . In all cases  $\sigma=0.005$ ,  $\Gamma_c=1$ ,  $\Gamma_h=2$ ,  $\tau_h=\tau_c=\tau_a=\tau_b=0.01$ ,  $T_c=100$ ,  $T_h=500$ , and  $w_h=100$ .

we mention the monotonic behavior of  $\bar{Q}_L$  with both  $z$  and  $\sigma$  while  $\epsilon$  is a convex function on  $z$  with progressively smaller values as the friction  $\sigma$  increases (when  $\sigma=0$ ,  $\epsilon$  is a monotonically increasing function on  $z$ ; see below). Figure 7(a) shows a two-dimensional plot of  $\bar{Q}_L$ ,  $\epsilon$ , and  $\Omega^{RE}$  for a constant  $\sigma (\neq 0)$  value, in which can be seen how the last two functions are convexlike with maxima for different  $z$  values. A straightforward consequence of the behavior of  $\epsilon$  and  $\bar{Q}_L$  is the parametric curve  $1/\epsilon$  versus  $1/\bar{Q}_L$  plotted in Fig. 7(b), characteristic of the all irreversible refrigeration cycles [1,15]. As in the work cycle, also  $z$  can be considered now as an appropriate independent variable in order to an optimization procedure of the COP,  $\epsilon$ , and  $\Omega^{RE}$ . The results are shown in Fig. 8(a) for the  $z$  values giving maximum COP,  $z_{max\epsilon}$ , and maximum  $\bar{\Omega}$ ,  $z_{max\bar{\Omega}}$  [under maximum heat absorbed  $z$  is identically null, see Figs. 6(a) and 7(a)]; Fig. 8(b) shows the maximum COP,  $\epsilon_{max}$ , and the COP at maximum  $\bar{\Omega}$ ,  $\epsilon_{max\bar{\Omega}}$  (the COP at maximum heat absorbed is again identically null); finally, Fig. 8(c) shows the (constant) maximum heat absorbed,  $Q_{L,max}$ , the heat absorbed at maximum COP,  $Q_{L,max\epsilon}$ , and at maximum  $\bar{\Omega}$ ,  $Q_{L,max\bar{\Omega}}$ . Note that under the  $\Omega$  performance regime also the refrigeration cycle presents values of the COP and heat absorbed which are intermediate

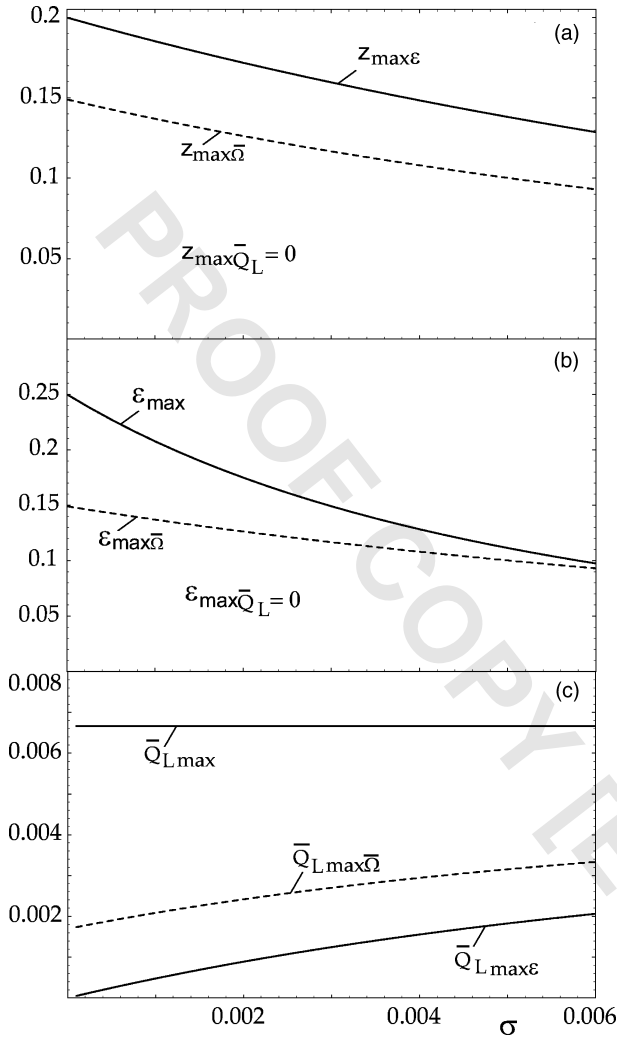


FIG. 8. Optimization results for the harmonic quantum refrigeration cycle: (a)  $z_{\max\bar{Q}_L}$ ,  $z_{\max\bar{\Omega}}$ , and  $z_{\max\epsilon}$ ; (b)  $\epsilon_{\max}$ ,  $\epsilon_{\max\bar{\Omega}}$ , and  $\epsilon_{\max\bar{Q}_L}$ ; (c)  $\bar{Q}_{L\max}$ ,  $\bar{Q}_{L\max\bar{\Omega}}$ , and  $\bar{Q}_{L\max\epsilon}$ . In all cases  $\Gamma_c=1$ ,  $\Gamma_h=2$ ,  $\tau_h=\tau_c=\tau_a=\tau_b=0.01$ ,  $T_c=100$ ,  $T_h=500$ , and  $w_h=100$ .

between those predicted by the maximum COP and maximum heat absorbed regimes.

When friction is absent ( $\sigma=0$ ) the COP monotonically decreases on  $z$  and, as a consequence, the  $1/\epsilon$  versus  $1/\bar{Q}_L$  plots are typical of an endoreversible limit [1,15]. However, this limit is only achieved when the conditions  $\sigma=0$  and high temperatures limit are both fulfilled [12]. In this limit we mention the value of the efficiency at maximum  $\Omega$ , which is given by the  $\tau$ -dependent expression  $\epsilon_{\max\bar{\Omega}}=\tau/(\sqrt{2-\tau}-\tau)$ , which (as expected) reproduces the corresponding value already reported for endoreversible Carnot-like, macroscopic refrigeration cycles with linear heat transfer laws [3].

### III. SUMMARY AND CONCLUDING REMARKS

We have presented a systematic study of the efficiency (COP) and work output (heat absorbed from the cold heat bath) for an irreversible, quantum harmonic heat engine (refrigerator) cycle when optimized under three different regimes: maximum efficiency (maximum COP), maximum work (maximum heat absorbed from the cold thermal bath), and one more which represents the tradeoff between energy benefits and losses for the specific job of the thermal device.

Beyond particular numerical values, it is interesting to face the obtained results for the harmonic quantum heat engine to those already reported for macroscopic, classic heat engines (with both linear and nonlinear heat transfer laws) [3,4] and for mesoscopic, stochastic, fluctuation rectifiers [3,5–7]. Independently of their dynamics, all power systems show as a significant characteristic that the maximum power and maximum efficiency regimes are close but noncoincident states. This fact gives rise to a looplike behavior for power-efficiency plots which is a specific sign of real motors. In regard to refrigeration systems, we stress the same qualitative behavior of the coefficient of performance and cooling power (the same parametric plots of the inverse of cooling power versus the inverse of the COP) both in the quantum and classical cases. Finally, and concerning the  $\Omega$  criterion of performance, we mention its intermediate character between those of maximum efficiency (COP) and maximum power output (cooling power), independent of the dynamics (classical, stochastic, or quantum mechanical) of the working medium.

In summary, heat engines (refrigerators) seem to show some similarities for the efficiency and power output (COP and cooling power) when studied in terms of appropriate independent variables in the context of finite time thermodynamics, independently of their nature and size. A unified analysis under different optimal performance regimes could give guidelines in order to design efficient energy converters and to compare their operation in different situations. In particular, and as noted by Greenspan [16], the optimization criteria based on a concrete *compromise* or *tradeoff* seem to be realistic in order to describe not only physical processes but also many human activities.

### ACKNOWLEDGMENTS

Financial support from Ministerio de Ciencia y Tecnología of Spain (Project No. BFM2002-01225 FEDER) and Junta de Castilla y León (Project No. SA080/04) are acknowledged. N. Sánchez appreciates a grant from Agencia Española de Cooperación Internacional (AECI) and from COFAA-IPN (México) during her stay at the University of Salamanca.

- [1] *Recent Advances in Finite-Time Thermodynamics*, edited by C. Wu, L. Chen, and J. Chen (Nova Science, New York, 1999).
- [2] R. S. Berry, V. A. Kazakov, S. Sieniutycz, Z. Szwast, and A. M. Tsirling, *Thermodynamics Optimization of Finite-Time Processes* (Wiley, Chichester, 2000).
- [3] A. Calvo Hernández, A. Medina, J. M. M. Roco, J. A. White, and S. Velasco, *Phys. Rev. E* **63**, 037102 (2001).
- [4] N. Sánchez Salas, S. Velasco, and A. Calvo Hernández, *Energy Convers. Manage.* **43**, 2341 (2002).
- [5] N. Sánchez Salas and A. Calvo Hernández, *J. Phys. D* **35**, 1442 (2002).
- [6] N. Sánchez Salas and A. Calvo Hernández, *Europhys. Lett.* **61**, 287 (2003).
- [7] N. Sánchez Salas and A. Calvo Hernández, *Phys. Rev. E* **68**, 046125 (2003).
- [8] V. A. Mironova, A. M. Tsirling, V. A. Kazakov, and R. S. Berry, *J. Appl. Phys.* **7**, 629 (1994).
- [9] R. Kosloff and T. Feldmann, *Phys. Rev. E* **65**, 055102 (2002).
- [10] B. Lin and J. Chen, *Phys. Rev. E* **67**, 046105 (2003); B. Lin, J. Chen, and B. Hua, *J. Phys. D* **36**, 406 (2003).
- [11] H. Saygin and A. Sisman, *J. Appl. Phys.* **90**, 3086 (2001).
- [12] T. Feldmann and R. Kosloff, *Phys. Rev. E* **61**, 4774 (2000).
- [13] E. Geva and R. Kosloff, *J. Chem. Phys.* **97**, 4398 (1992).
- [14] L. A. Arias-Hernández and F. Angulo-Brown, *J. Appl. Phys.* **81**, 2973 (1997).
- [15] J. M. Gordon and K. C. Ng, *Cool Thermodynamics* (Cambridge International Science Publishing, Cornwall, 2000).
- [16] N. S. Greenspan, *Nature (London)* **409**, 137 (2001).